BMC Plant Biology

RESEARCH Open Access

Metabolomic study of *Cynara cardunculus* L. growing at different altitudes reveals the flowering stage as the balsamic time

Manuela Mandrone[1], Ilaria Chiocchio[1*], Simona Trincia[1], Antonio De Agostini[2,3], Cinzia Sanna[2] and Ferruccio Poli[1]

Abstract

Background *Cynara cardunculus* L. is a low-input crop increasingly relevant in semi-arid regions due to its resilience, ecological value, and versatility. It provides nutraceutical, pharmaceutical, and industrial applications due to its richness in bioactive compounds, particularly cynaropicrin, caffeoylquinic acids, and flavonoids. It has been suggested that the crop should be moved preferentially to marginal environments at higher altitudes, giving greater biomass productivity. However, while environmental conditions are known to influence crop performance, the effects on the plant's metabolome remain underexplored. Hence, this study investigates how altitudinal gradients and phenological stages shape the leaf metabolic profile of wild *C. cardunculus* populations, with the aim of identifying key adaptive metabolic responses and determining the optimal harvest period for herbal use.

Results By means of Proton Nuclear Magnetic Resonance (^{1}H NMR)-based metabolomics, supported by two dimensional NMR and Mass spectrometry analyses, we found that cynaropicrin, a key bioactive compound, increases during the flowering stage and in response to high temperatures. Similarly, chiro-inositol, reported here for the first time in *C. cardunculus*, was also more abundant at the flowering stage. In contrast, leaves at the pre-flowering stage were enriched in amino acids (proline, valine, phenylalanine), sucrose, and luteolin-malonyl hexoside. As for the altitude, we found that leaves collected from plants growing below 300 m a.s.l. showed the highest accumulation of aromatic compounds before flowering, while at the flowering stage the leaf metabolome was more homogeneous across the different collection sites.

Conclusions In conclusion, the results of this work support the flowering stage as the balsamic time of *C. cardunculus*. Indeed, leaves collected at this phenological stage, yield a more consistent metabolite profile, enriched in chiro-inositol and cynaropicrin. Moreover, this study confirms the suitability of high-altitude cultivation without compromising the production of key bioactive compounds.

Keywords ^{1}H NMR metabolomics, Wild cardoon, Food supplement, Stress-response, Cynaropicrin, Chiro-inositol

*Correspondence:
Ilaria Chiocchio
ilaria.chiocchio2@unibo.it
[1]Department of Pharmacy and Biotechnology (FaBit), Alma Mater Studiorum, University of Bologna, Via Irnerio 42, Bologna 40126, Italy
[2]Department of Life and Environmental Sciences, University of Cagliari, Via S. Ignazio da Laconi 13, Cagliari 09123, Italy
[3]Agricultural Research Agency of Sardinia (AGRIS), Viale Trieste 111, Cagliari 09123, Italy

Background

As a relatively low-input crop for biofuel and biodiesel production [1, 2], *Cynara cardunculus* L. (Asteraceae family) is becoming increasingly important in semi-arid regions [3]. *C. cardunculus* is resilient in marginal lands with minimal agricultural inputs [4], representing a strategy to counteract erosion and improve soil fertility. The species supports carbon sequestration [5], integrates well into arable crop systems, and yields bio-based products while avoiding competition with food crops. Moreover, it resists well to salinity stress, and has a potential role in phytoremediation, due to its capability to uptake and translocate heavy metals [4].

C. cardunculus is a robust perennial plant characterized by large spiny leaves and branched flowering stems. It is native to the Mediterranean basin, where it grows spontaneously in uncultivated areas [6].

As documented by Acquadro et al. [7], *C. cardunculus* complex was first classified into three distinct botanical taxa: the wild perennial cardoon (*C. cardunculus* var. *sylvestris* (Lamk) Fiori), the cultivated leafy cardoon (*C. cardunculus* var. *altilis* DC.), and the globe artichoke (*C. cardunculus* subsp. *scolymus* Hegi). Today, following the most recent taxonomic revision, *C. cardunculus* var. *altilis* and *C. cardunculus* var. *sylvestris* are synonymous with *Cynara cardunculus* L., while the globe artichoke is classified as *Cynara scolymus* L [8].

The largest number of scientific articles is focused on the globe artichoke (*C. scolymus*), due to its economic relevance as a food crop, cultivated globally, with a particular prevalence in Southern Europe [9]. However, it should be pointed out that, due to the repeated taxonomic revisions, the scientific literature on *C. cardunculus* is often confusing, making it difficult to discern the studies concerning the wild species from those regarding the cultivated ones.

The wild cardoon originates from southwestern Europe, North Africa, and western Turkey, and it has been recognized as the progenitor of both the cultivated leafy cardoon and the globe artichoke [10]. Unlike the widely cultivated globe artichoke, cardoon cultivation is limited to Spain, Italy, southern France, and Greece, where its young leaves, which represent the edible portion, are eaten in traditional cuisine or prepared in the form of decoction/infusion for the liver and blood-purifying, digestive, antispasmodic and diuretic properties [11–14]. Moreover, due to their high content of aspartic proteases, specifically cardosins A and B, its dried flowers are used as a milk coagulant in the production of traditional cheeses [6].

As highlighted also by the ethnobotany, *C. cardunculus* has a versatility that goes beyond its use as an energy crop with high biomass production. It, in fact, has several other industrial applications ranging from nutraceuticals [15, 16] to less conventional uses such as pulp paper and natural dying [17].

The species, in addition to its nutritional value and characteristic flavor, is rich in bioactive compounds [18, 19], and seen the importance that *C. cardunculus* is gaining for botanicals, the Committee on Herbal Medicinal Products (HMPC) of the European Medicines Agency (EMA) recognized preparations from *C. cardunculus* leaves as herbal remedies for the symptomatic relief of digestive disorders [20].

The most characteristic active principles of the species are cynaropicrin, cynarin (1,3-*O*-dicaffeoylquinic acid), and cynaroside (luteolin-7-*O*-glucoside) [21, 22]. Among them, cynaropicrin is the most abundant guaianolide-type sesquiterpenes lactone, which confers a typical bitter taste [9]. This compound has been studied for its anti-inflammatory, antimicrobial, antitumoral [23], and anti-hyperlipidemic activities [24], and it is considered a promising natural product to treat hepatitis C virus infection [25]. Cynarin is a caffeoylquinic acid derivative, commonly found in this species together with other metabolites of the same class, such as: chlorogenic acid (5-*O*-caffeoylquinic acid), and 1,5-*O*-dicaffeoylquinic acid [26]. As it is known, both caffeoylquinic acids and flavonoids are important bioactive compounds contributing to the health-promoting properties of *C. cardunculus*, and, in particular, cynaroside is recognized for its antimicrobial, antileishmanial, hepatoprotective, antidiabetic, anti-inflammatory, and anticancer activities [27].

Ierna et al. [3] suggested the opportunity to move the crop from plain to the marginal environment located at a higher altitude, which is generally characterized by higher average annual rainfall, yielding greater productivity in biomass and seeds. Nevertheless, the impact of the hydroclimatic differences on plant metabolome has not been studied yet. Thus, a better understanding of the metabolomic behavior of *C. cardunculus* in response to environmental factors, and different phenological phases, would be relevant both to understand the crop adaptation strategies and in terms of bioprospecting studies. In fact, it is important to acquire data on any changes in the amount and ratio of the most abundant primary and secondary metabolites produced by this species when subjected to different growth conditions. In addition, for the development of herbal products, it is relevant to know when the active principle(s) in the leaf is/are maximized (balsamic period).

In this frame, the present study was designed to investigate how environmental factors associated with altitudinal gradients and phenological stages influence the leaf metabolome of *C. cardunculus* in natural populations. Using an untargeted ^{1}H NMR-based metabolomic approach supported by UHPLC-UV-MS, we aimed to (i) characterize the main primary and specialized

metabolites of wild populations, (ii) assess the metabolic changes occurring between pre-flowering (Pre-FL) and flowering (FL) stages, and (iii) evaluate the relationships between key metabolites and hydroclimatic parameters. We hypothesized that phenology and environmental variation would significantly affect the abundance of selected metabolites, with potential implications for crop adaptation strategies and for identifying the balsamic time, namely the optimal harvesting period for herbal uses.

Methods

Chemicals

Deuterium oxide (D_2O, 99.90% D) and Deuterated methanol (CD_3OD, 99.80% D) were purchased from Eurisotop (Cambridge Isotope Laboratories, Inc, France). All other chemicals were purchased from Merck KGaA (Darmstadt, Germany).

Plant material and collection

Leaves of *Cynara cardunculus* L. were collected in 2018 at two time points, Pre-FL and FL, the first indicating the phenological state before flowering (April) and the latter referring to the phenological status coinciding with flowering (June). In accordance with the phenological stages classification of *C. cardunculus* proposed by Archontoulis [28], Pre-FL corresponds to stage 4, while FL corresponds to stage 6. Plant material was sampled, in accordance with local legislation, from five locations in Sardinia Island as reported in Fig. 1. The sites where the plant material was harvested are not included in national or local parks or any other natural protected areas. No specific permission is required to collect all samples described in this study.

Within each collection site, leaves were harvested from 10 different individuals and then pooled. After sampling, the fresh plant material was dried in a ventilated stove at 40 °C to constant weight. Species were botanically identified by Prof. Cinzia Sanna, and voucher specimens were preserved in the General Herbarium of the Department of Life and Environmental Sciences, University of Cagliari (*Herbarium* CAG) with the voucher codes CAG 790/v1-v5.

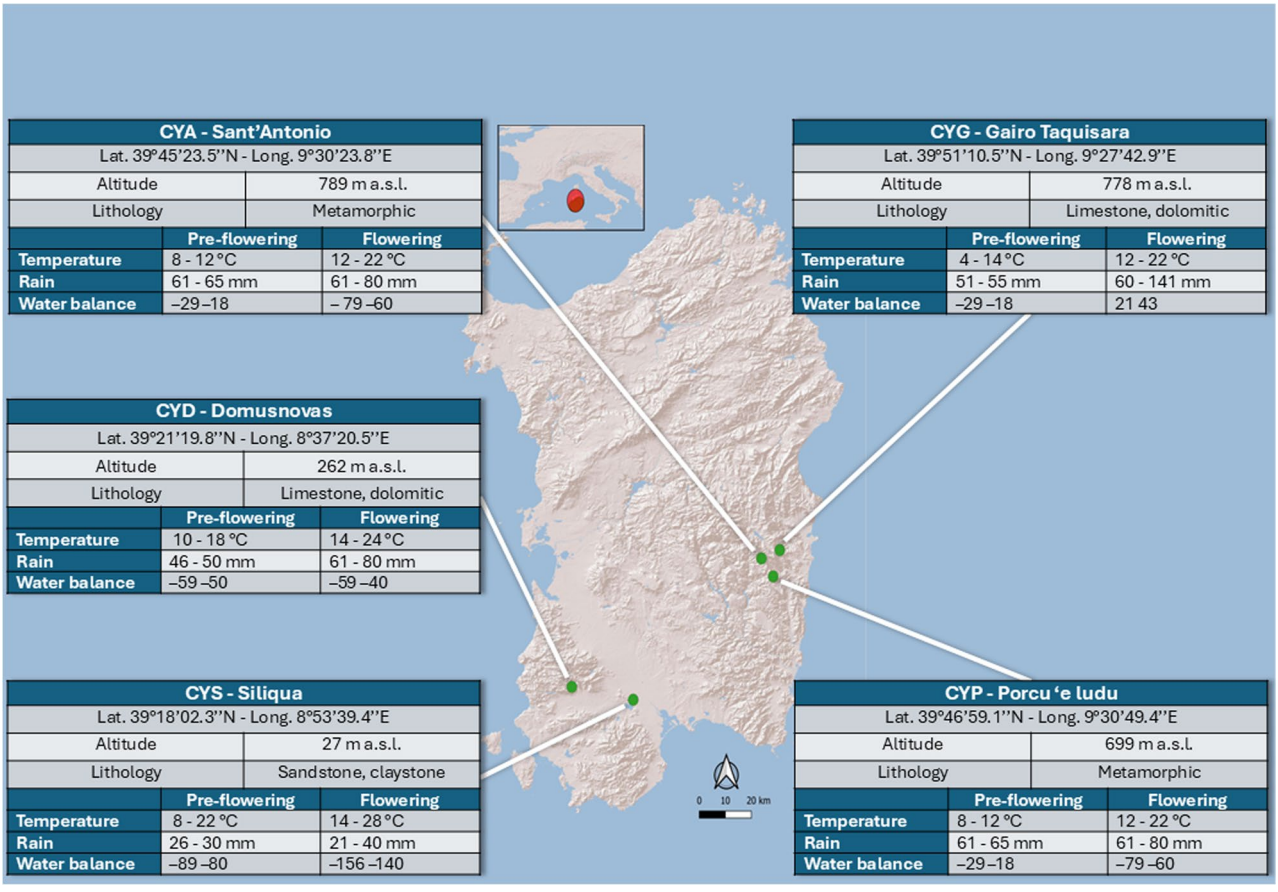

Fig. 1 Geographical and climatological features of collection sites. For each site GPS coordinates, altitude (m above sea level, a.s.l.), and lithological framework are reported. Mean temperature (° C), precipitations (mm), and water balance are reported as minimum and maximum values recorded in all collection sites and both phenological stages

Plant metabolome, apart from genetic factors, is largely determined by the environment in which plants grow, since functional metabolites are produced to answer a variety of ecological tasks. In accordance with the objectives of this study, and specifically to document the relationships between key metabolites in *C. cardunculus* and environmental parameters, the five sampling sites were chosen to represent diversified ecological growing contexts both from the hydroclimatic and the pedo-lithological viewpoint. Sampling sites were consequently selected to maximise the diversity of environmental conditions while presenting coinciding phenological stages in the studied plants (i.e., Pre-FL and FL). Sampling sites were also chosen at an adequate distance from each other to exclude the eventuality of hybridization among populations and also due to their pristine conditions, to exclude the anthropic factor from confounding the experimental results. The sites which resulted suitable to be included in the present study are located at altitudes ranging between 27 and 789 m above sea level (a.s.l.), and also different in terms of average minimum and maximum temperature (T min e T max), precipitations (mm of rain), and water balance (intended as the ratio between potential evapotranspiration and the amount of rainfall, representative of water availability for the plant). Hydroclimatic data were obtained from the database of the regional agency for environmental protection in Sardinia (ARPAS) for the year 2018 [29] and are reported in Fig. 1.

Sample preparation for ^{1}H NMR profiling

Extracts, chemical analysis, and biological assays were performed between 2018 and 2020. Samples for ^{1}H NMR profiling were prepared using 300 mg of plant material and as solvents 10 mL of a 50:50 mixture of MeOH and H_2O, then sonicated for 30 min and subsequently centrifuged (1400 rpm, RCF = 110 *g*) for 10 min. An aliquot of 800 µl of the supernatant was separated from the pellet and dried in vacuum concentrator (SpeedVac SPD 101b 230, Savant, Italy). Each dried extract was weighted and then resolubilized in 800 µl (50:50) of MeOH-d_4 and phosphate buffer (90 mM, pH 6.0) in H_2O-d_2 containing 0.01% of the standard trimethylsilylpropionic-2,2,3,3-d_4 acid sodium salt (TMSP), directly transferred in NMR tubes and subjected to ^{1}H NMR profiling.

NMR analysis

^{1}H NMR, homonuclear (COSY and J resolved) and heteronuclear 2D correlation experiments (HMBC, HSQC) were recorded at 25 °C on a Bruker Avance Ascend 600 instrument equipped with autosamplers and a cryoprobe Prodigy. For ^{1}H NMR profiling, the instrument operated at ^{1}H NMR frequency of 600.13 MHz, and CD_3OD was used as internal lock. Each ^{1}H NMR spectrum consisted of 46 scans with a relaxation delay (RD) of 2 s and spectral width of 9595.8 Hz (corresponding to δ 16.0), the measurement lasted 4 min. A presaturation sequence (PRESAT) was used to suppress the residual water signal at δ 4.83.

The spectra were manually phased, and baseline corrected, and calibrated to the internal standard trimethyl silyl propionic acid sodium salt (TMSP) at δ 0.0 using Mestrenova software (Mestrelab Research, Spain). TMSP was also used as a standard for semi-quantitative analysis of identified metabolites, performed by peak area integration respectively to the internal standard.

The molar ratio (M*x*/M*y*) between each metabolite *x* and the internal standard *y*, was determined using Eq. 1 [30]:

$$Mx \,/\, My \;=\; (Ix \,/\, Iy) \;\times\; (Ny \,/\, Nx) \tag{1}$$

Where *M* represents the molarity, *I* the integrated signal area in the spectrum and *N* the number of nuclei responsible for the NMR signal.

Metabolite concentration (Table S1) was expressed both as mg of metabolite per g of plant dried weight (DW) according to Eq. 2, and as mg of metabolite per g of dried extract (DE) according to Eq. 3.

$$\begin{aligned}&\text{mg of metabolite/g DW}\\&\quad = M * (\text{MW}/300 * 0.8) * 1000\end{aligned} \tag{2}$$

where M represents the molarity as determined by NMR.

$$\begin{aligned}&\text{mg of metabolite/g DE}\\&\quad = M * (\text{MW}/\text{EC}) * 1000\end{aligned} \tag{3}$$

where EC represents the calculated concentration of each analysed extract (mg of dried extract/0.8 mL).

The ratio of cynaropicrin, chiro-inositol, and luteolyn malony-hexoside abundance between Pre-FL and FL was also expressed as fold change (fc) calculated as: concentration (mg/g DE) at FL / concentration (mg/g of DE) at Pre-FL.

The analysis of ^{1}H NMR profiles of extracts was performed based on an in-house library and comparison with literature [31, 32].

UHPLC-UV-ESI-MS analysis

The extraction procedure for UHPLC-MS analysis was analogous to the one used for NMR analysis with the difference of using not-deuterated solvents. Thirty mg of plant material underwent ultrasound assisted extraction using 1 ml of methanol 50%. After centrifugation (10 min, 1700 *g*) the supernatant was directly analysed. Each sample was extracted three times to perform three independent analyses.

UHPLC – MS analyses were run on a Waters ACQUITY ARC UHPLC/MS system consisting of a QDa mass spectrometer equipped with an electrospray ionization interface and a 2489 UV/Vis detector. The detected wavelengths (l) were 254 nm and 340 nm. The analyses were performed on an XBridge BEH C18 column (100 mm × 2.1 mm i.d., particle size 2.5 µm) with a XBridge BEH C18 VanGuard Cartridge precolumn (5 mm × 2.1 mm i.d., particle size 1.8 µm). For each sample 4 µL were injected and eluted with the following mobile phase: H_2O (0.1% formic acid) (A) and MeCN (0.1% formic acid) (B). The following gradient was used: 0–0.78 min, 5% B; 0.78–7.50 min, 5 – 20% B; 7.50–10.00 min, 20–70% B; 10.00–11.50 min, 70% B; 11.50–12.50 min, 70 – 5% B; 12.50–14.00 min, 5% B. Flow rate: 0.8 mL/min. Electrospray ionization in positive and negative modes was applied in the mass scan range 50 – 1200 Da. The most intense *m/z* values under each chromatographic peak were considered for the annotation of the compounds.

Multivariate data analysis and statistics

For multivariate analysis, spectral intensities were reduced to integrated regions of equal width (δ 0.04) and the data were normalized by total area using Mestrenova software (Mestrelab Research, Spain). The regions at δ 4.85–4.75 and 3.33–3.30 were excluded from the analysis because of the residual solvent signals. Data were further subjected to Pareto scaling and the models (PCA, OPLS-DA, OPLS) were developed using SIMCA software (v. 18.0, Umetrics, Sweden) as reported in Mandrone et al. [33].

Supervised models were evaluated by the goodness of fit (R^2x (cum) and R^2y(cum)) and goodness of prediction (Q^2(cum)), together with the parameters given by cross validation tests: permutation test (performed using 200 permutations) and Cross Validation Analysis of Aariance (CV-ANOVA) (Table S2). The significance of the variables in each model was evaluated by their variable influence on projection (VIP) scores, giving priority to variables having VIP scores higher than 1. To develop the OPLS models, the mean temperature and the mean water balance were calculated for each location at the Pre-FL and FL and used as *y* variables.

The abundance of the compounds detected by UHPLC-UV-ESI-MS was evaluated by integrating the area of the chromatographic peaks, performing three independent experiments, and the values were expressed as mean value ± standard deviation (SD). Statistical analysis was performed using Graph Pad Prism 10 software (La Jolla, CA). Samples at different locations and phenological stages were compared by two-way analysis of variance (ANOVA) with Tukey post-hoc test, considering differences at p values < 0.05 significant.

Results and discussion

The first analytical step was the elucidation of the ^{1}H NMR profiles of the samples (Fig. 2), functional to the interpretation of the results given by multivariate data analysis.

Several primary metabolites, such as fatty acids, amino acids (alanine, proline, asparagine, phenylalanine), organic acids (succinic, malic, and formic acid), sugars (sucrose, α-glucose and β-glucose), and chiro-inositol were identified (Fig. 2; Table S3) by their diagnostic signals in the ^{1}H NMR spectra, and subsequentially semi-quantified (Table S1).

The presence of chiro-inositol has already been documented in *Cynara scolymus* L. (globe artichoke) [34], and in this work, we identify this metabolite, for the first time, also in *C. cardunculus.* Notably, chiro-inositol was one of the most abundant primary metabolites in all samples (Table S1). This information is relevant for the valorization of *C. cardunculus* leaves as an ingredient for industrial herbal products with specific biological activities, particularly given the proven ability of chiro-inositol to regulate hormonal levels in various clinical disorders [35], leading to a growing interest in recovering this health-promoting metabolite from agricultural products and by-products [36–38].

As for specialized metabolites, the sesquiterpene lactone cynaropicrin and the alkaloid trigonelline were detected in the samples, along with several aromatic compounds whose signals were visible in the spectra. By performing *J*-resolved experiments, it was confirmed that these aromatic signals were due to flavonoids and caffeic acid derivatives (Figure S1). Due to the high degree of overlap of these spectral signals, it was not possible to fully elucidate their molecular structures directly by NMR profiling. Thus, the most abundant phenolics and flavonoids present in the samples were annotated by further UHPLC-UV-ESI-MS analysis (with detection at λ = 340 nm). This analysis allowed us to tentatively identify six compounds: three flavanols (luteolin, luteolin malonyl-hexoside, and cynaroside) and three caffeoyl quinic acid derivatives (cynarin, caffeoylquinic acid, and succinyl-dicaffeoylquinic acid) (Fig. 3; Table 1). Based on their ratio, cynaroside and luteolin malonyl-hexoside were also putatively identified in the ^{1}H NMR profiles (Figure S1).

Once the ^{1}H NMR profiles were elucidated, the differences between the samples were explored by metabolomics. The PCA (Figure S2) differentiated the samples harvested in Pre-FL from those harvested in FL. Hence, this difference was better explored by OPLS-DA, using as a discriminant class the phenological stage of the plant (Pre-FL and FL) (Fig. 4).

Besides the metabolomic changes occurring from Pre-FL to FL, we also investigated whether environmental

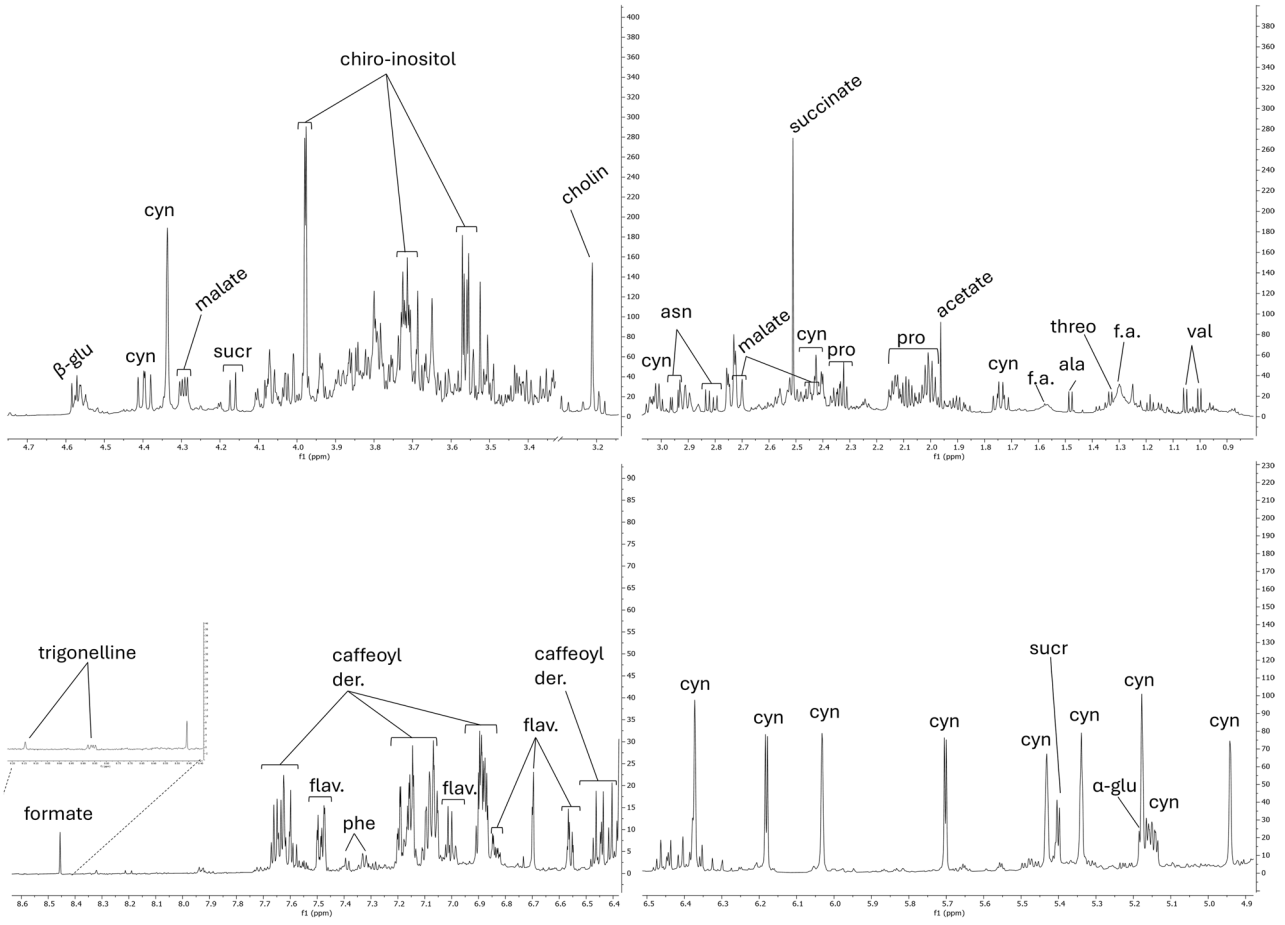

Fig. 2 Elucidated ^{1}H NMR spectrum of a representative sample of *C. cardunculus* (CYG-FL). Extended spectral regions. Top: spectral regions from δ 0.8 to 3.1 and from δ 3.2 to 4.7. Bottom: spectral regions from δ 4.9 to 6.5. and δ from 6.4 to 8.6; α-glu = α-glucose, β-glu = β-glucose, ala= alanine, asn= asparagine, caffeoyl der.= caffeoyl derivatives, cyn= cynaropicrin, f.a.= fatty acids, flav.= flavonoids (cynaroside and luteolin malonyl-hexoside), phe= phenylalanine, pro= proline, sucr= sucrose, threo= threonine, val= valine

parameters could correlate with specific metabolomic variations by building three independent OPLS models (using in turn as *y* variable: altitude, mean water balance (W), and mean temperature (T), respectively) (Figure S3), and a final comprehensive model based on all three *y* variables (3*y*-OPLS) (Fig. 5).

As a result, the S-Plot of the OPLS-DA model (Fig. 4C), indicated that FL was mainly characterized by increasing concentration of fatty acids (VIP = 1.09) and two important bioactive compounds, namely chiro-inositol (VIP = 2.54) and cynaropicrin (VIP = 1.33). Cynaropicrin and chiro-inositol increased as T raised (found by OPLS with *y* = T (Figure S3) and confirmed by 3*y*-OPLS in Fig. 5). Obviously, the general increase in temperature is related to seasonality, which directly affects plant development. Thus, an increase in cynaropicrin and chiro-inositol concentration should be interpreted in the light of both a transition from Pre-FL to FL and an increase in temperature.

Scavo et al. [39] found that cynaropicrin content in *C. cardunculus* leaves was maximized in April compared to November and January. However, while their investigation ended with plants at Pre-FL, our results show that cynaropicrin keeps increasing as the plant blooms (at FL). More in detail, by ^{1}H NMR semi-quantitative analysis (Table S1), the content of cynaropicrin from Pre-FL to FL shifts from mean values of 0.5% to 1.6% (w/w of dry plant material). Noteworthy, the calculated fold change (*fc*) of this metabolite in the extracts, from Pre-FL to FL, was especially high in one location, namely CYD (*fc* = 6.6), while for the other samples *fc* was a value between 1.8 and 3.7.

The increase of both chiro-inositol and cynaropicrin at FL might occur to accomplish a protective role under stressful abiotic conditions.

Cyclitols, including chiro-inositol, have been regarded as osmoprotectants in plants [40, 41]. Although no direct studies have specifically addressed the role of chiro-inositol in plants, other isomers such as myo-inositol and

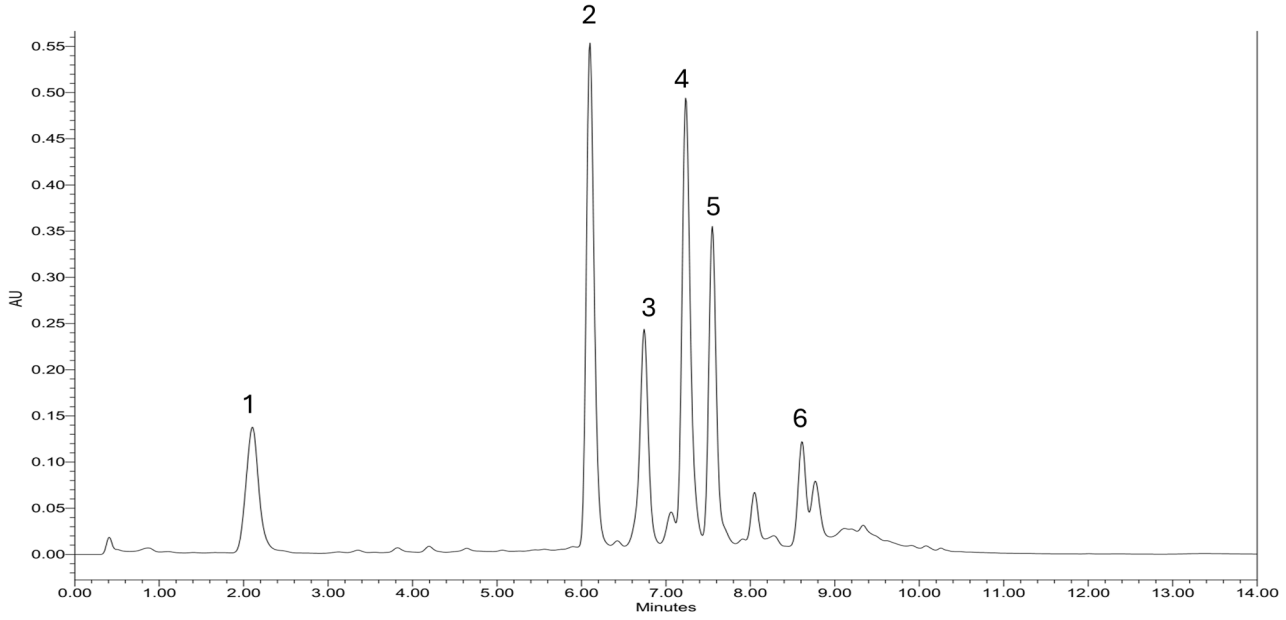

Fig. 3 UHPLC-UV-ESI-MS chromatogram (at λ 340 nm) of CYP-Pre-FL. The eluting molecules were putatively characterized based on the *m/z* values (see Table 1): 1 = caffeoylquinic acid, 2 = cyaroside, 3 = cynarin, 4 = succinyl-dicaffeoylquinic acid, 5 = luteolin malonyl-hexoside, 6 = luteolin

Table 1 Specialized metabolites tentatively identified by UHPLC-UV-ESI-MS and experimental values obtained in both positive (ESI+) and negative (ESI-) ionization modes. Numbers in the first column correspond to the same compounds of Fig. 3 and follow the elution order

	Compound	R_t (min)	Molecular Formula	Exact mass (u)	Experimental m/z in ESI^+	Experimental m/z in ESI^-
1	Caffeoylquinic acid	2.12	$C_{16}H_{18}O_9$	354.0951	355.13 $[M+H]^+$	353.23 $[M-H]^-$
2	Cynaroside	6.09	$C_{21}H_{20}O_{11}$	448.1006	449.26 $[M+H]^+$	447.06 $[M-H]^-$
3	Cynarin	6.76	$C_{25}H_{24}O_{12}$	516.1268	517.18 $[M+H]^+$	515.38 $[M-H]^-$
4	Succinyl-dicaffeoylquinic acid	7.26	$C_{29}H_{28}O_{15}$	616.1428	617.30 $[M+H]^+$	616.00 $[M]^-$
5	Luteolin malonyl- hexoside	7.55	$C_{24}H_{22}O_{14}$	534.1010	535.28 $[M+H]^+$	533.06 $[M-H]^-$
6	Luteolin	8.76	$C_{15}H_{10}O_6$	286.0477	287.11 $[M+H]^+$	285.11 $[M-H]^-$

pinitol have been found to increase in response to temperature stress. For instance, in *Medicago sativa* cyclitol levels were significantly higher in plants grown under summer conditions compared to spring [42], while in *Glycine max* elevated concentrations of cyclitols were reported under combined water deficit and high-temperature stress [43].

Lahuta and Dzik [44], and Lombardo et al. [45] found that cynaropicrin accumulated in *C. cardunculus* leaves under stress conditions (stimulated by external application of gibberellic acid). Hence, increasing temperature could be considered a stressor with an effect on the accumulation of both metabolites. However, direct evidence for heat or drought-induced cynaropicrin accumulation in plants is still lacking. On the other hand, cynaropicrin is a protective compound responsible for the bitter taste that repels chewing insects [46], thus, its production is also reasonably maximized during the FL, when the plant strives to protect the flower.

To maximize the content of cynaropicrin and chiro-inositol in *C. cardunculus* leaf-based herbal products, it is not only necessary to understand the plant's protective responses to increasing temperatures but also to identify the plant's developmental phase with the highest concentration of these compounds. While FL was characterized by increasing cynaropicrin and chiro-inositol, the OPLS-DA indicated that proline (VIP = 3.79), sucrose (VIP = 2.72), and valine (VIP = 1.30) were more concentrated in Pre-FL than FL (Fig. 4C). As initially suggested by the OPLS-DA (Fig. 2B), the 3*y*-OPLS (Fig. 5) confirmed that samples inhabiting altitudes lower than 300 m a.s.l. (CYS and CYD) and samples growing at altitudes higher than 300 m a.s.l. (CYA, CYP, CYG) clustered separately in both Pre-FL and FL. The environmental explanation for this can be found in the fact that, in both Pre-FL and FL, as to be expected, a negative correlation exists among altitude and temperature (higher altitudes are featured by lower temperatures, Fig. 6A), conversely, a positive correlation can be found (during FL) between altitude and W (higher altitudes are featured by increased water availability, Fig. 6B). Lower sites resulted, in conclusion, characterized by higher temperatures and lower

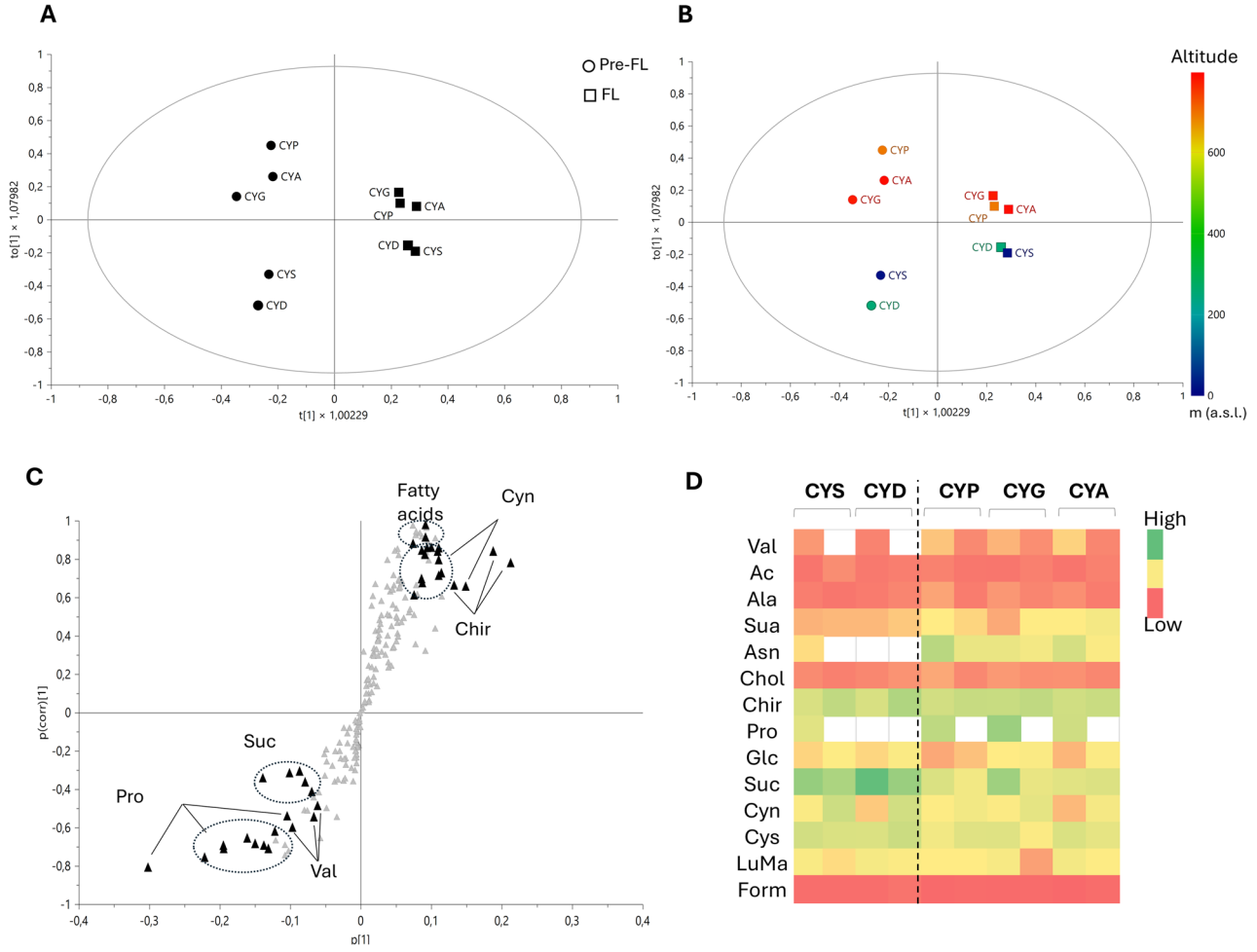

Fig. 4 Metabolomic analysis. OPLS-DA built using as *x* variables bucketed ^{1}H NMR spectra and phenological stage as discriminant class (**A**) Score Scatter Plot, with the two classes represented by dots (Pre-FL) and squares (FL), (**B**) observations (samples) colored according to altitude (following a color gradient from blue (27 m a.s.l) to red (789 m a.s.l.)), (**C**) S-plot of the OPLS-DA, triangles are bucketed ^{1}H NMR signals, black ones are signals of the metabolites contributing more to the class differentiation, up right is representative of FL and bottom left of Pre-FL. **D** Heatmap displaying the variation on individual metabolites from Pre-FL to FL in all locations, from the lowest (CYS; CYD) to the highest. Gradient of concentration (mg/g DE) decreases from green to red (white = not detected).Val =valine, Ac= acetic acid, Ala= alanine, Sua= Succinic acid, Asn= Asparagine, Chol= coline, Chir= Chiro-inositol, Pro=proline; Glc = *β*-glucose, Sucr= sucrose, Cyn= cynaropicrin, Cys=cynaroside, LuMA=luteolin malonyl-hexoside, Form=formic acid

W if compared to the higher sites, both factors exacerbating the growing conditions for plants inhabiting lower altitudes. This is also confirmed by the fact that the metabolomic differences were more pronounced in Pre-FL (Figs. 4B and 5), when the positive correlation of altitude and W was strong and significant.

According to the analysis of the Bi-Plot of the 3*y*-OPLS (Fig. 5), the metabolomic difference between Pre-FL at lowest altitudes and Pre-FL at highest altitudes was given by caffeoylquinic derivatives and sucrose, which resulted more concentrated in Pre-FL at lowest altitudes, and by primary metabolites (proline, asparagine, valine, phenylalanine, alanine, choline, malic acid), which resulted more concentrated in Pre-FL at highest altitudes (see also Fig. 4D). The accumulation of high levels of osmoprotectants, such as proline and choline, suggests an adaptive response to abiotic constraints associated with high-altitude environments. Although osmolytes are generally associated with drought or osmotic stress, they also accumulate under cold-induced metabolic stress due to secondary dehydration, oxidative damage, and possibly mild hypoxic conditions in the rhizosphere related to low temperatures, high humidity, and reduced oxygen diffusion [47].

Moreover, the accumulation of asparagine, in particular, may be a storage form of nitrogen under conditions of limited growth and protein synthesis [48].

Conversely, the metabolomic pattern of low-altitude populations, which experience higher temperatures and reduced water availability, may reflect increased carbon flux toward energy storage (sugars) and antioxidant compound synthesis as a protective mechanism against

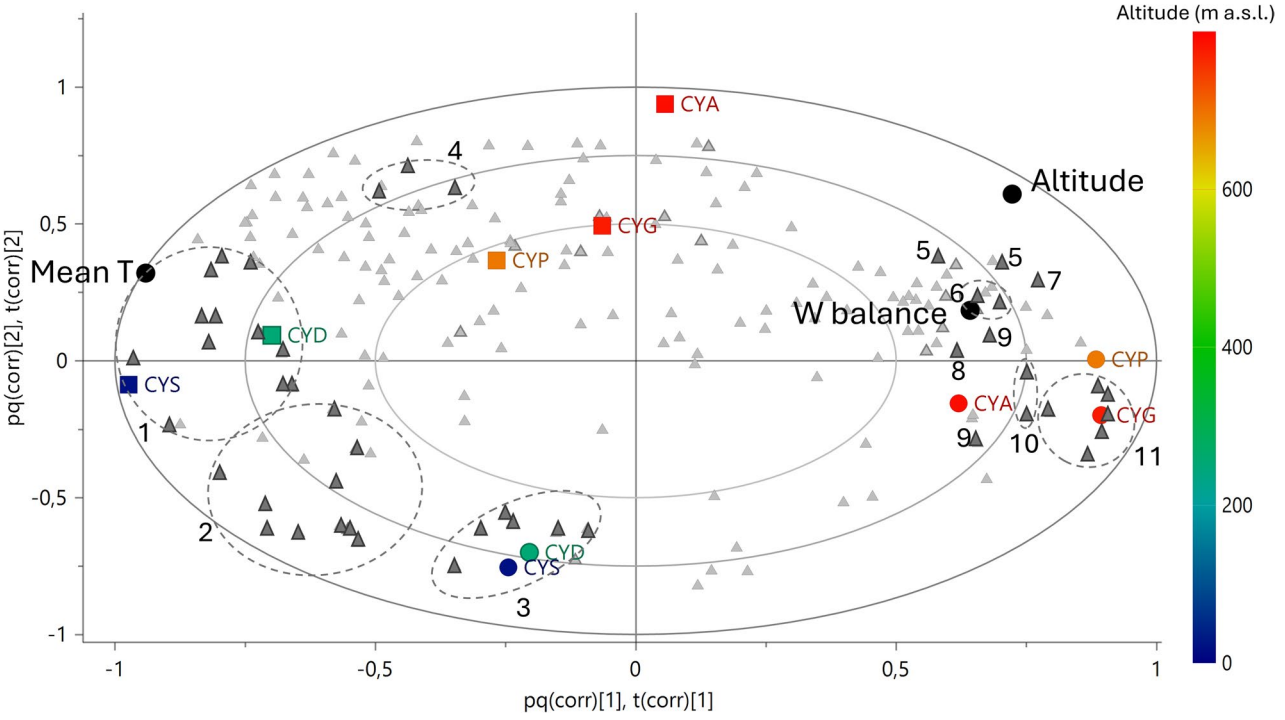

Fig. 5 Bi-Plot of 3*y*-OPLS model built using as *x* variables (grey triangles) the bucketed ^{1}H NMR spectra, and as *y* variables (black dots) altitude, mean temperature (Mean T), and water balance (Mean W) for each location. Sample is colored according to altitude; dots = Pre-FL, squares = FL; 1 = cynaropicrin (VIP = 1.3); 2 = caffeoyl derivatives (VIP = 1.62); 3 = sucrose (VIP = 1.85); 4 = chiro-inositol (VIP = 1.72); 5 = malic acid (VIP = 2.03); 6 = asparagine (VIP = 1.48); 7 = alanine (VIP < 1); 8 = choline (VIP = 1.17); 9 = phenylalanine (VIP < 1); 10 = valine (VIP = 1.48); 11 = proline (VIP = 3.33). The metabolites with VIP > 1 contribute the most to the differentiation of the samples

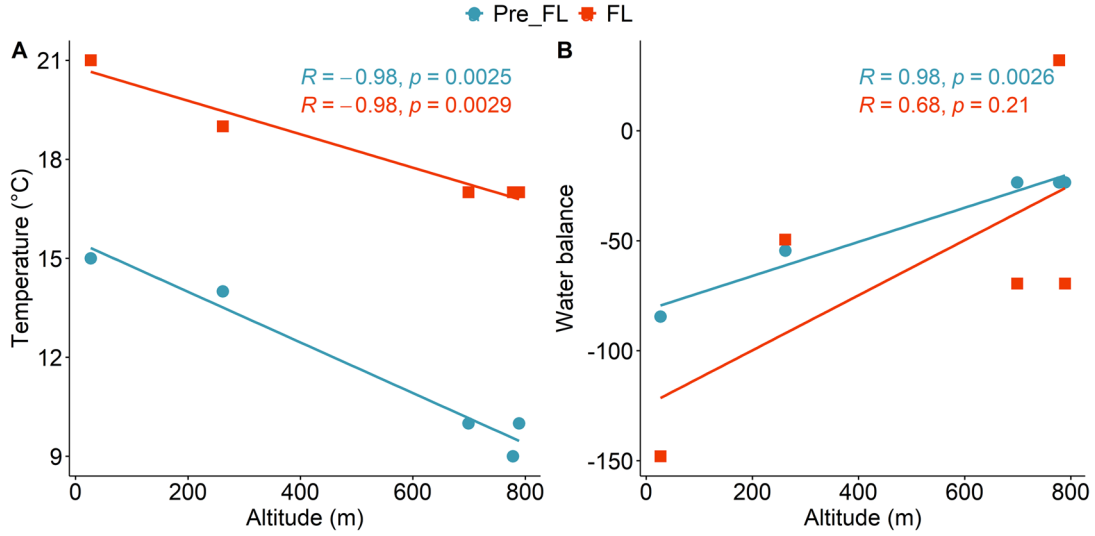

Fig. 6 Scatterplot of values of altitude (m) in relation to (**A**) temperature (°C), and in relation to (**B**) Water balance (W) during Pre-FL (blue line) and FL (red line). Pearson test was implemented to assess statistical significance of the correlation (significant at $p < 0.05$)

heat and drought-induced oxidative stress. The slightly higher level of chiro-inositol at low altitudes suggests the predominant involvement of this metabolite in osmoprotection in response to drought. In addition to the information obtained by ^{1}H NMR metabolomics, a more in-depth analysis of the aromatic profile was performed using UHPLC-UV-ESI-MS data, which allowed for further comparison between the samples. As displayed in Fig. 7, at the lowest-altitude site (CYS), the aromatics significantly decreased during FL (Fig. 7). This pattern is consistent with NMR metabolomics data, which revealed higher aromatic content at Pre-FL in the lowest-altitude

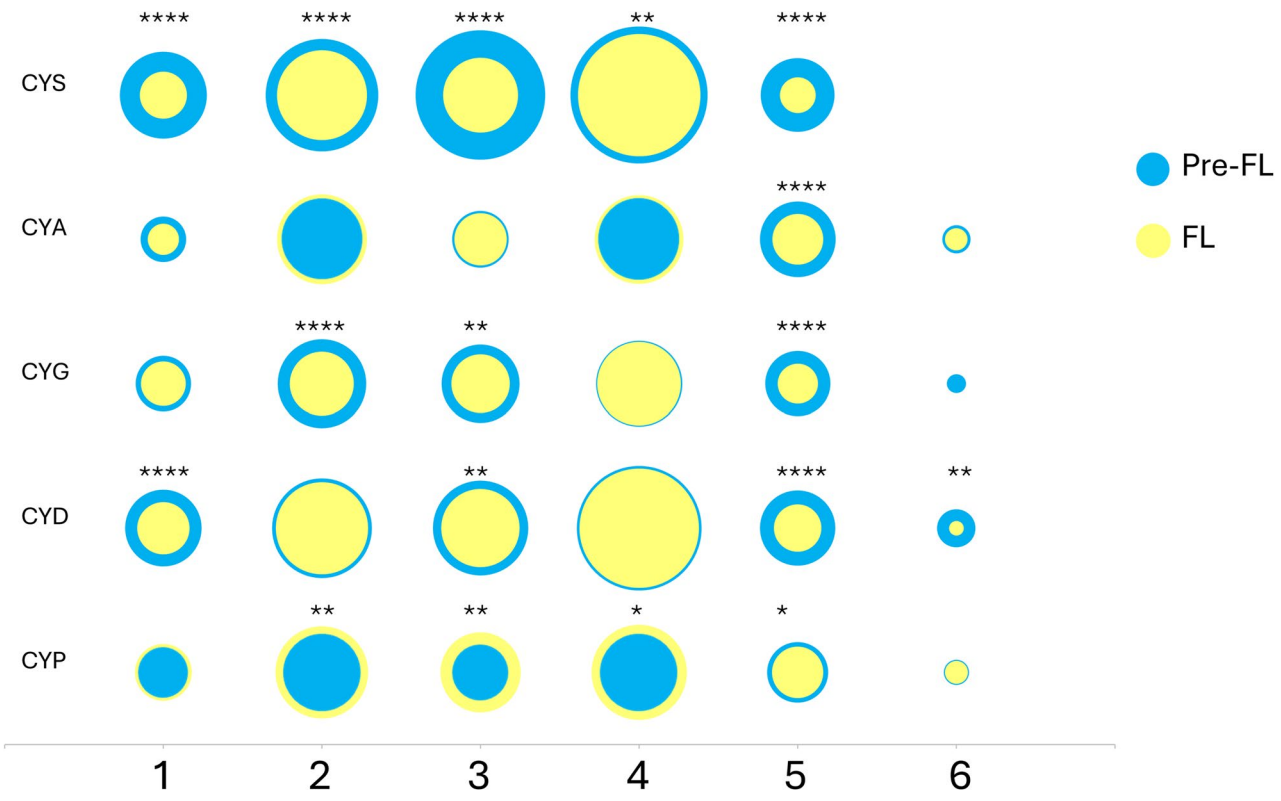

Fig. 7 Bubble plot showing the content of flavonoids and caffeoyl derivatives detected by UHPLC-UV-ESI-MS analysis in *C. cardunculus* samples in the two phenological stages (Pre-FL= blue, FL= yellow) and in the five different locations (indicated by the labels). The area of the bubbles represents the area of the integrated chromatographic peaks at λ 340 nm reduced by 50%. Compounds (from left to right) follow the elution order of the chromatographic analysis. 1 = caffeoylquinic acid, 2 = cynaroside, 3 = cynarin, 4 = succinyl-dicaffeoylquinic acid, 5 = luteolin malonyl-hexoside, 6 = luteolin. Asterisks indicate significant differences between Pre-FL and FL (in the same population) of $p < 0.05$ (*); $p < 0.01$ (**); $p < 0.005$ (***); $p < 0.0001$ (****) according to two-way ANOVA test

sites (CYS and CYD) compared to the highest-altitude sites (Figure S4).

Luteolin malonyl-hexoside was the only aromatic compound showing significant variation in all the locations from Pre-FL to FL (see asterisks in Fig. 7). Its concentration decreased at FL with a high statistical significance ($p < 0.0001$) except in CYP where it decrease from Pre-FL to FL with a lower level of statistical significance ($p < 0.05$). CYP was uniquely characterized by a significant increase in cynarin. Notably, CYP is a high-altitude site that experienced the sharpest rise in maximum temperatures between Pre-FL and FL (a 10 °C excursion), reinforcing the idea that temperature is a crucial driver of the *C. cardunculus* metabolome.

Malonylated flavonoid glycosides are recognized vacuolar storage forms; the general decline in luteolin malonyl-hexoside from Pre-FL to FL likely reflects a phenology-dependent reallocation of resources and adjustments in flavonoid conjugation/sequestration, possibly compounded by co-varying environmental factors (UV radiation, temperature, water status), growth dilution, and tissue dynamics. During flowering, carbon and reducing power are typically redirected from leaf secondary metabolism to reproductive growth, often resulting in reduced accumulation of certain flavone conjugates in leaves [49]. Clarifying the mechanisms underlying their turnover will require targeted enzymatic and transcriptomic assays, as well as flux-based analyses.

Conclusions

The overall results of this work further support the valorization of *Cynara cardunculus* leaves as an ingredient for health-promoting botanical products, as they contain not only cynaropicrin and aromatic compounds (either flavonoids or caffeoyl derivatives) but also chiro-inositol. Furthermore, by showing that cynaropicrin and chiro-inositol differentially accumulate in the leaf depending on the phenological phase, we identified the flowering stage as the balsamic period. This is also the last phenological stage in which it is possible to collect leaves from *C. cardunculus* before they become senescent. The preferential accumulation of cynaropicrin and chiro-inositol observed in our results appears to be a response to increasing temperatures and water deficit. This is likely due to the role of these metabolites in providing the plant with enhanced resistance to abiotic stressors and adverse

climatic factors. The aromatic compounds were more sensitive to hydroclimatic differences between locations during the Pre-FL. During FL, however, they were more uniform despite the collection site. This further suggests that flowering is the optimal harvest time for the leaves to ensure a more consistent metabolite profile in the product, independently of the collection site.

Luteolin malonyl-hexoside is the only exception; if the goal is to specifically maximize its concentration, harvesting leaves during the pre-flowering stage, potentially from plants at lower altitudes, might be recommended. Demonstrating that the plant metabolome is largely similar across altitudes, especially at flowering, this work further supports the potential to favor cultivating this crop in marginal, high-altitude environments. Based on our results, these areas offer greater biomass yield without a significant decrease in bioactive compounds.

Future studies including multi-year sampling, larger population sets, and extended environmental data (i.e. detailed soil physicochemical properties) would provide a more comprehensive picture of the ecological drivers of metabolic variation in *C. cardunculus.*

Abbreviations

a.s.l.	Above sea level
CV-ANOVA	Cross Validation Analysis of Variance
ESI-MS	Electrospray Ionization-Mass Spectrometry
fc	Fold change
FL	Flowering stage
NMR	Nuclear Magnetic Resonance
OPLS	Orthogonal Projections to Latent Structures
OPLS-DA	Orthogonal Partial Least Squares Discriminant Analysis
PCA	Principal Component Analysis
Pre-FL	Pre-flowering stage
TMSP	Trimethylsilylpropionic-2,2,3,3-d_4 acid sodium salt
UHPLC-UV	Ultra-High-Performance Liquid Chromatography-Ultraviolet Detection
VIP	Variable Influence on Projection

Supplementary Information

The online version contains supplementary material available at https://doi.org/10.1186/s12870-026-08782-6.

Supplementary Material 1.

Acknowledgements

Authors thank Antonio Cellini and Francesca Bugamelli (University of Bologna) for UHPLC-MS analysis, and Immacolata Maresca (University of Ferrara) for technical support.

Authors' contributions

Data curation: IC, MM; Formal analysis: ADA, IC and ST; Funding acquisition: FP; Investigation: ADA, CS, IC, MM, Methodology: IC, MM; Supervision: FP, MM; Validation: IC, MM, CS; Roles/Writing - original draft: IC, CS, MM; Writing - review & editing: MM, IC. All authors read and approved the final manuscript.

Funding

This research did not receive any specific grant from funding agencies in the public, commercial, or not-for-profit sectors.

Data availability

The NMR spectra and the dataset generated during the current study are available in the Zenodo repository (10.5281/zenodo.15518787).

Declarations

Ethics approval and consent to participate

Not applicable.

Competing interests

The authors declare no competing interests.

Received: 27 October 2025 / Accepted: 14 April 2026
Published online: 29 April 2026

References

1. Angelini. Long-term evaluation of biomass production and quality of two cardoon (Cynara cardunculus L.) cultivars for energy use. Biomass Bioenergy. 2009;33(5):810–6.
2. Mancini M, Bresó A, Federico R, Lanza Volpe M, Leskovar D, Cravero V. Biomass Characterization of Wild and Cultivated Cardoon Accessions and Estimation of Potential Biofuels Production. SSRN Electron J. 2022.
3. Ierna A, Sortino O, Mauromicale G, Biomass. Seed and Energy Yield of Cynara cardunculus L. as Affected by Environment and Season. Agronomy. 2020;10(10):1548.
4. Pappalardo HD, Toscano V, Puglia GD, Genovese C, Raccuia SA. Cynara cardunculus L. as a Multipurpose Crop for Plant Secondary Metabolites Production in Marginal Stressed Lands. Front Plant Sci. 2020;11.
5. Neri U, Pennelli B, Simonetti G, Francaviglia R. Biomass partition and productive aptitude of wild and cultivated cardoon genotypes (Cynara cardunculus L.) in a marginal land of Central Italy. Ind Crops Prod. 2017;95:191–201.
6. Sales-Gomes M, Lima-Costa ME. Immobilization of Endoproteases from Crude Extract of Cynara cardunculus L. Flowers. Food Sci Technol Int. 2008;14(3):271–6.
7. Acquadro A, Lanteri S, Scaglione D, Arens P, Vosman B, Portis E. Genetic mapping and annotation of genomic microsatellites isolated from globe artichoke. TAG Theor Appl Genet Theor Angew Genet. 2009;118(8):1573–87.
8. The WFO Plant List | World Flora Online. https://wfoplantlist.org/plant-list/. Accessed 29 November 2023.
9. Ramos PAB, Santos SAO, Guerra ÂR, Guerreiro O, Freire CSR, Rocha SM, et al. Phenolic composition and antioxidant activity of different morphological parts of Cynara cardunculus L. var. altilis (DC). Ind Crops Prod. 2014;61:460–71.
10. Gatto A, De Paola D, Bagnoli F, Vendramin GG, Sonnante G. Population structure of Cynara cardunculus complex and the origin of the conspecific crops artichoke and cardoon. Ann Bot. 2013;112(5):855–65.
11. Le piante nella. tradizione popolare della Sardegna (Aldo Domenico Atzei) - Carlo Delfino editore. 2003.
12. Loi MC, Poli F, Sacchetti G, Selenu MB, Ballero M. Ethnopharmacology of ogliastra (villagrande strisaili, sardinia, Italy). Fitoterapia. 2004;75(3–4):277–95.
13. Christaki E, Bonos E, Florou-Paneri P. Nutritional and functional properties of cynara crops (Globe Artichoke and Cardoon) and their potential applications: A Review. Int J Appl Sci Technol. 2012;2:64–70.
14. Chiocchio I, Marincich L, Mandrone M, Trincia S, Tarozzi C, Poli F. Saving the local tradition: ethnobotanical survey on the use of plants in Bologna district (Italy). J Ethnobiol Ethnomed. 2024;20(1):33.
15. Zayed A, Serag A, Farag MA. Cynara cardunculus L.: Outgoing and potential trends of phytochemical, industrial, nutritive and medicinal merits. J Funct Foods. 2020;69:103937.
16. Borroni M, Pozzi CM, Daniotti S, Gatto F, Re I. Multi-Criteria Decision-Making Approach for Nutraceuticals Greener Applications: The Cynara cardunculus Case Study. Sustainability. 2021;13(23):13483.
17. Gominho J, Lourenço A, Curt M, Fernández J, Pereira H. Characterization of hairs and pappi from Cynara cardunculus capitula and their suitability for paper production. Ind Crops Prod. 2009;29(1):116–25.
18. Gominho J, Curt MD, Lourenço A, Fernández J, Pereira H. Cynara cardunculus L. as a biomass and multi-purpose crop: A review of 30 years of research. Biomass Bioenergy. 2018;109:257–75.

19. Barracosa P, Barracosa M, Pires E. Cardoon as a Sustainable Crop for Biomass and Bioactive Compounds Production. Chem Biodivers. 2019;16(12):e1900498.
20. Cynarae folium -. herbal medicinal product | European Medicines Agency (EMA). https://www.ema.europa.eu/en/medicines/herbal/cynarae-folium. Accessed 17 June 2025.
21. Mandim F, Pinela J, Marcelino S, Dias MI, Barracosa P, Ivanov M, et al. Insights into the phenolic composition and in vitro bioactivity of cardoon capitulum: A nutraceutical-oriented valorization study. Food Chem. 2024;435:137480.
22. Ramos PAB, Ferro AM, Oliveira MM, Gonçalves S, Freire CSR, Silvestre AJD, et al. Biosynthesis and bioactivity of Cynara cardunculus L. guaianolides and hydroxycinnamic acids: a genomic, biochemical and health-promoting perspective. Phytochem Rev. 2019;18(2):495–526.
23. Mandim F, Santos-Buelga C, C F R Ferreira I, Petropoulos SA, Barros L. The wide spectrum of industrial applications for cultivated cardoon (Cynara cardunculus L. var. Altilis DC.): A review. Food Chem. 2023;423:136275.
24. Shimoda H, Ninomiya K, Nishida N, Yoshino T, Morikawa T, Matsuda H, et al. Anti-hyperlipidemic sesquiterpenes and new sesquiterpene glycosides from the leaves of artichoke (Cynara scolymus L.): structure requirement and mode of action. Bioorg Med Chem Lett. 2003;13(2):223–8.
25. Elsebai MF, Mocan A, Atanasov AG. Cynaropicrin: A Comprehensive Research Review and Therapeutic Potential As an Anti-Hepatitis C Virus Agent. Front Pharmacol. 2016;7:472.
26. Ciancolini A, Alignan M, Pagnotta MA, Vilarem G, Crinò P. Selection of Italian cardoon genotypes as industrial crop for biomass and polyphenol production. Ind Crops Prod. 2013;51:145–51.
27. Bouyahya A, Taha D, Benali T, Zengin G, El Omari N, El Hachlafi N, et al. Natural sources, biological effects, and pharmacological properties of cynaroside. Biomed Pharmacother. 2023;161:114337.
28. Archontoulis Sv, Struik Pc, Vos J, Danalatos N. g. Phenological growth stages of Cynara cardunculus: codification and description according to the BBCH scale. Ann Appl Biol. 2010;156(2):253–70.
29. ARPAS, IMC - Riepiloghi mensili. https://www.sar.sardegna.it/pubblicazioni/riepiloghimensili/mensili.asp. Accessed 17 June 2025.
30. Bharti SK, Roy R. Quantitative 1H NMR spectroscopy. TrAC Trends Anal Chem. 2012;35:5–26.
31. de Falco B, Incerti G, Amato M, Lanzotti V. Artichoke: botanical, agronomical, phytochemical, and pharmacological overview. Phytochem Rev. 2015;14(6):993–1018.
32. Liu X, Grieve C. Accumulation of Chiro-inositol and Other Non-structural Carbohydrates in Limonium Species in Response to Saline Irrigation Waters. J Am Soc Hortic Sci. 2009;134(3):329–36.
33. Mandrone M, Chiocchio I, Barbanti L, Tomasi P, Tacchini M, Poli F. Metabolomic Study of Sorghum (Sorghum bicolor) to Interpret Plant Behavior under Variable Field Conditions in View of Smart Agriculture Applications. J Agric Food Chem. 2021;69(3):1132–45.
34. Hernández-Hernández O, Ruiz-Aceituno L, Sanz ML, Martínez-Castro I. Determination of Free Inositols and Other Low Molecular Weight Carbohydrates in Vegetables. J Agric Food Chem. 2011;59(6):2451–5.
35. Gambioli R, Forte G, Aragona C, Bevilacqua A, Bizzarri M, Unfer V. The use of D-chiro-Inositol in clinical practice. Eur Rev Med Pharmacol Sci. 2021;25(1):438–46.
36. Ruiz-Aceituno L, García-Sarrió MJ, Alonso-Rodriguez B, Ramos L, Sanz ML. Extraction of bioactive carbohydrates from artichoke (Cynara scolymus L.) external bracts using microwave assisted extraction and pressurized liquid extraction. Food Chem. 2016;196:1156–62.
37. Mena-García A, Rodríguez-Sánchez S, Ruiz-Matute AI, Sanz ML. Exploitation of artichoke byproducts to obtain bioactive extracts enriched in inositols and caffeoylquinic acids by Microwave Assisted Extraction. J Chromatogr A. 2020;1613:460703.
38. Ingallina C, Di Matteo G, Spano M, Acciaro E, Campiglia E, Mannina L, et al. Byproducts of Globe Artichoke and Cauliflower Production as a New Source of Bioactive Compounds in the Green Economy Perspective: An NMR Study. Mol Basel Switz. 2023;28(3):1363.
39. Scavo A, Rial C, Varela RM, Molinillo JMG, Mauromicale G, Macias FA. Influence of Genotype and Harvest Time on the Cynara cardunculus L. Sesquiterpene Lactone Profile. J Agric Food Chem. 2019;67(23):6487–96.
40. Kopecká R, Kameniarová M, Černý M, Brzobohatý B, Novák J. Abiotic Stress in Crop Production. Int J Mol Sci. 2023;24(7):6603.
41. Xu Y, Fu X. Reprogramming of Plant Central Metabolism in Response to Abiotic Stresses: A Metabolomics View. Int J Mol Sci. 2022;23(10):5716.
42. Ratiu IA, Al-Suod H, Ligor M, Monedeiro F, Buszewski B. Effects of growth conditions and cultivability on the content of cyclitols in Medicago sativa. Int J Environ Sci Technol. 2021;18(1):33–48.
43. Vital RG, Müller C, Freire FBS, Silva FB, Batista PF, Fuentes D, et al. Metabolic, physiological and anatomical responses of soybean plants under water deficit and high temperature condition. Sci Rep. 2022;12(1):16467.
44. Lahuta LB, Dzik T. d-chiro-Inositol affects accumulation of raffinose family oligosaccharides in developing embryos of Pisum sativum. J Plant Physiol. 2011;168(4):352–8.
45. Lombardo S, Scavo A, Pandino G, Cantone M, Mauromicale G. Improvement in the Cynaropicrin, Caffeoylquinic Acid and Flavonoid Content of Globe Artichokes with Gibberellic Acid Treatment. Plants Basel Switz. 2022;11(14):1845.
46. Eljounaidi. Accumulation of cynaropicrin in globe artichoke and localization of enzymes involved in its biosynthesis. Plant Sci. 2015;239:128–36.
47. Behr JH, Bouchereau A, Berardocco S, Seal CE, Flowers TJ, Zörb C. Metabolic and physiological adjustment of Suaeda maritima to combined salinity and hypoxia. Ann Bot. 2017;119(6):965–76.
48. Lea PJ, Sodek L, Parry MAJ, Shewry PR, Halford NG. Asparagine in plants. Ann Appl Biol. 2007;150(1):1–26.
49. Liu Y, Huang X, Chong X, Huang S, Yu C, Yu H, et al. Transcriptomics Integrated with Metabolomics Reveals the Accumulation Mechanism of Flavones in Jinsi Huangju. Horticulturae. 2025;11(8):948.

Publisher's note